SYNCHROTRON BEAM-LOADING STABILITY WITH A HIGHER RF HARMONIC*

Tai-Sen F. Wang

AT-7, MS H825, Los Alamos National Laboratory
Los Alamos, New Mexico 87545, USA

Abstract

This work extends Robinson's stability studies [1] to include a higher rf harmonic. Using an equivalent circuit model, the stability of the "0-mode" coherent dipole oscillation of bunched beams is studied for synchrotrons or storage rings with rf systems operated at the fundamental and a higher harmonic, i.e., a second or third harmonic. Analytical expressions of the stability criteria are derived from the linearized circuit equations. Numerical solutions of the fully nonlinear equations are provided to compare with the analytical results. A simple feedback model for stabilization is discussed.

I. INTRODUCTION

Higher-harmonic rf systems are frequently used in synchrotrons and storage rings to increase bunch length in order to reduce the space charge effects, and to damp the longitudinal instability by increasing the synchrotron frequency spread [2,3]. Under the circumstance of heavy beam-loading, instability may occur due to the beam-induced voltage on the cavities. For a single-frequency rf system, this kind of instability has been well studied [1,4]. However, few documents can be found on the theory of the stability of rf systems with higher harmonics [3,5]. A rigorous study of this subject requires either complex calculations using kinetic theory and nonlinear particle dynamics or substantial computer simulations for exploring the parameter space. Because some future accelerators may use a higher-harmonic rf system, a theoretical understanding of and methods for estimating the stability of double-harmonic rf system are needed before rigorous theory and computational data become available. Simple conditions for stability were obtained by Miyahara et al. [3]; however, these results are applicable for some specific cases only. In the followings, we discuss the beam loading stability in an rf system with a higher harmonic by directly investigating the equations derived from the equivalent circuit model. An example of controlling the system stability by using the "rf feedback" [6] will be given. Details of the mathematical derivations and part of the following materials have been included in a few recent reports [7,8].

II. THEORETICAL MODEL

*Work supported by the US Department of Energy, Office of High Energy and Nuclear Physics.

In the equivalent circuit model, an rf cavity is envisioned as a parallel RLC circuit. The applied rf power source and the circulating beam current can be modeled as currents i_g and i_b, respectively. We consider a system having two cavities: a "fundamental cavity" operated at the frequency ω_1, which is equal to the hth harmonic of the revolution frequency of beam particles, and a "harmonic cavity" operated at the frequency ω_2, which is equal to $n\omega_1$. For systems run with both frequencies of rf power in one type of cavity, the following formalism still is applicable.

By Kirchhoff's law, the total voltage on each cavity v_k satisfies the differential equation

$$\frac{d^2v_k}{dt^2}+2\alpha_k\frac{dv_k}{dt}+\omega_{rk}^2v_k=2\alpha_k\mathcal{R}_k\frac{d(i_{gk}+i_b)}{dt} \quad , \tag{1}$$

where $k = 1$ (for the fundamental cavity) or 2 (for the higher harmonic cavities); t is the time, $\alpha_k = \omega_{rk}/(2Q_k)$, $\omega_{rk}^2 = 1/(L_kC_k)$; $\mathcal{R}_k$, L_k, C_k and Q_k are the shunt resistance, the inductance, the capacitance, and the quality factor of each cavity respectively. For high-Q cavities, only those Fourier components of i_b with frequencies near ω_{rk} need to be considered. In the steady state, v_k is maintained at the phase ψ_{vk} with respect to the beam current. Our interest here is the stability of the small oscillations of the phase deviations in cavity voltages ϕ_{vk} and beam current ϕ_{bk} ($\phi_{b2} = n\phi_{b1}$) around their steady states. Thus, making the substitutions of $v_k = V_k(t)\exp\{-j[\omega_kt+\psi_{vk}+\phi_{vk}(t)]\}$, $i_b \approx I_{b1}\exp\{-j[\omega_1t+\phi_{b1}(t)]\}+I_{b2}\exp\{-j[\omega_2t+\phi_{b2}(t)]\}$, and $i_{gk} = I_{gk}\exp\{-j(\omega_kt+\psi_{gk})\}$ in Eq. (1), we derive

$$\frac{1}{\alpha_k}\frac{dV_k}{dt}+V_k=\mathcal{R}_k\left[I_{gk}\cos\phi_{vk}-I_{bk}\cos(\phi_{bk}-\phi_{vk}-\psi_{vk})\right] \quad , \tag{2}$$

and

$$\frac{1}{\alpha_k}\frac{d\phi_{vk}}{dt}=\frac{\omega_{r1}-\omega_{gk}}{\alpha_k}-\mathcal{R}_k\left[I_{gk}\sin\phi_{vk}+I_{bk}\sin(\phi_{bk}-\phi_{vk}-\psi_{vk})\right]/V_k \quad , \tag{3}$$

where $j=\sqrt{-1}$. Some approximations were used to derive Eqs. (2) and (3). First, we assumed that the bandwidths of the impedances of these two types of cavities are much smaller than the separation between their resonant frequencies, so only one of the beam current's harmonics is considered for each cavity. Second, because $\alpha_k \ll \omega_k$ for high-Q and high frequency cavities, we neglected the time derivatives of V_k and dV_k/dt when comparing with the products of these qunatities and the rf frequencies. For simplicity, we assumed $\psi_{gk} = \psi_{vk}$, i.e., the system is tuned for the rf sources to see *real* impedances. In obtaining Eq. (3), we also used the approximation $\omega_k + \omega_{rk} \approx 2\omega_k$.

The equations of beam motion are those of synchrotron motion:

$$\frac{d\Delta E}{dt} = \frac{q\omega_1}{2\pi h}\left[V_1 \sin(\psi_{s1} + \phi_{v1} - \phi_{b1}) - V_{s1}\sin\psi_{s1} + V_2\sin(\psi_{s2} + \phi_{v2} - n\phi_{b1}) - V_{s2}\sin\psi_{s2}\right] \quad , \tag{4}$$

and

$$\frac{d\phi_{b1}}{dt} = -\frac{\eta\omega_1}{\beta^2}\left(\frac{\Delta E}{E_o}\right) \quad , \tag{5}$$

where E_o is the total energy of the reference particle, ΔE is the energy deviation from E_o, β is the speed of the reference particle divided by the speed of light, ψ_{sk} is the synchronous angle between the beam current and the cavity voltages, V_{sk} is the value of V_k at steady state, and $\eta = \gamma_t^{-2} - \gamma^{-2}$. In this paper we consider the case of $\gamma < \gamma_t$. However, the case of $\gamma > \gamma_t$ can be treated with the same procedures. Note that in the steady state $V_{sk} = \mathcal{R}_k(I_{gk} - I_{bk}\cos\psi_{vk})$, and

$$-(\mathcal{R}_k I_{bk}\sin\psi_{vk})/V_{sk} = (\omega_{rk} - \omega_k)/\alpha_k = \tan\phi_{yk}, \tag{6}$$

where ϕ_{yk} is referred to as the detuning angle.

III. LINEAR STABILITY CONDITIONS

Applying Routh's criteria [9], we obtain the following necessary and sufficient conditions for a stable system:

$$F_1 = b_0 > 0,$$
$$F_2 = b_3(b_4b_5 - b_3) - b_5(b_5b_2 - b_1) > 0,$$
$$F_3 = (b_4b_5 - b_3)(b_2b_3 + b_0b_5 - b_1b_4) - (b_2b_5 - b_1)^2 > 0,$$

and

$$F_4 = [b_3(b_4b_5 - b_3) - b_5(b_5b_2 - b_1)][b_1(b_2b_5 - b_1) - b_0b_3b_5] - [b_1(b_4b_5 - b_3) - b_0b_5^2]^2 > 0,$$

where

$$b_0 = \omega_s^2(1-\xi)\rho_1\rho_2 - \lambda_1\rho_2 - \lambda_2\rho_1,$$
$$b_1 = 2\omega_s^2(1-\xi)(\alpha_1\rho_2 + \alpha_2\rho_1) - 2(\alpha_1\lambda_2 + \alpha_2\lambda_1),$$
$$b_2 = \rho_1\rho_2 + \omega_s^2(1-\xi)(\rho_1 + \rho_2 + 4\alpha_1\alpha_2) - \lambda_1 - \lambda_2,$$
$$b_3 = 2(\alpha_1\rho_2 + \alpha_2\rho_1) + 2\omega_s^2(1-\xi)(\alpha_1 + \alpha_2),$$
$$b_4 = \rho_1 + \rho_2 + 4\alpha_1\alpha_2 + \omega_s^2(1-\xi),$$
$$b_5 = 2(\alpha_1 + \alpha_2),$$
$$\xi = -(nV_{s2}\cos\psi_{s2})/(V_{s1}\cos\psi_{s1}),$$
$$\lambda_k = (\alpha_k^2\omega_s^2\mathcal{R}_k I_{bk}\tan\phi_{yk})/(V_{s1}\cos\psi_{s1}),$$
$$\rho_k = \alpha_k^2\sec^2\phi_{yk},$$

where $\omega_s = [(-q\eta h V_{s1}\cos\psi_{s1})/(2\pi m R^2)]^{1/2}$, is the synchrotron frequency without the higher harmonic rf field; q and m are the charge and the relativistic mass of a beam particle respectively; and R is the averaged machine radius. All these conditions must be satisfied for the system stability. Condition $F_1 > 0$ can be rewritten as

$$\frac{I_{b1}\mathcal{R}_1}{V_{s1}\cos\psi_{s1}} < \frac{2(1-\xi)}{\sin(2\phi_{y1}) - n\vartheta(\mathcal{R}_2/\mathcal{R}_1)\sin(2\phi_{y2})} \quad , \tag{7}$$

where $\vartheta = I_{b2}/I_{b1}$. Equation (7) is similar to the result obtained by Miyahara et al. [3] except for the factor of ϑ on the right hand side. When $\xi = \vartheta = 0$, the above inequality reduces to the Robinson stability criterion [1]

$$\sin(2\phi_{y1}) < (2V_{s1}\cos\psi_{s1})/(\mathcal{R}_1 I_{b1}) \quad . \tag{8}$$

The other Robinson stability condition, $\sin\phi_{y1} > 0$, can be obtained from the condition $F_4 > 0$ by letting $\xi = \vartheta = 0$ and $\alpha_2 \to 0$.

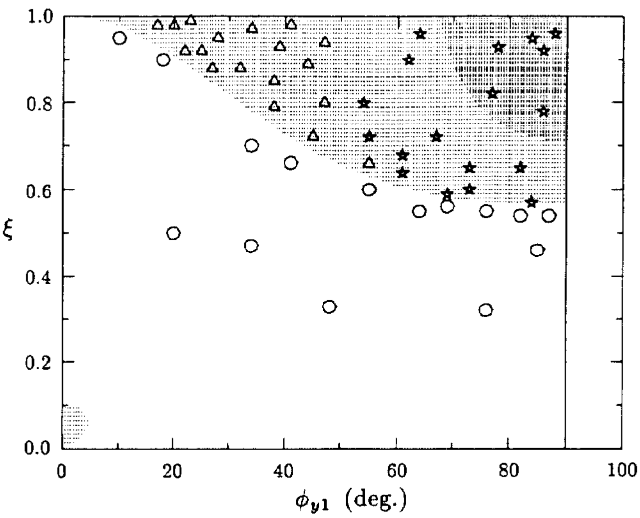

Figure 1. Comparison of the analytical and the numerical solutions for Eqs. (2)–(5). Shaded areas correspond to the unstable regions: $F_4 > 0$ at the lower left corner; $F_1 > 0$ and $F_4 > 0$ (heavily shaded) at the upper right corner. Numerical solutions of Eqs. (2)–(5) are shown by circles for stable and damped oscillations, stars for unbounded unstable solutions, and triangles for initially unstable but asymptotically bounded solutions.

The nonlinear equations (2)–(5) have been solved numerically to compare with the results evaluated from the linear stability conditions. In general, solutions of Eqs. (2)–(5) can be roughly grouped into three categories: (i) stable and damped oscillations, (ii) unbounded unstable solutions, and (iii) initially unstable but asymptotically bounded solutions. A comparison of the numerical with the analytical solutions is given in Figure 1. In this case, both the fundamental and second harmonic rf are used for bunching. The unstable zones are shown in the shaded areas on the ξ - ϕ_{y1} plane for the parameter values of $n = 2$, $\psi_{s1} = 0$, $\psi_{s2} = \pi$, $(\omega_s/\alpha_1)^2 = 0.1$, $\mathcal{R}_2/\mathcal{R}_1 = 0.3$, $Q_1 = Q_2$, and $\vartheta = 0.7$. The cavity detunings are related by $\tan\phi_{y2} = -(n\vartheta\mathcal{R}_2/\xi_1)\tan\phi_{y1}$. Conditions $F_2 > 0$ and $F_3 > 0$ are always satisfied in this region. Also shown in Figure 1 are the qualitative results of more than fifty numerical solutions of Eqs. (2)–(5). The agreements between the analytical and the numerical solutions seem very good in describing the local stability.

IV. FEEDBACK CONTROL

We consider an example of increasing stability by using the "rf feedback" [6]. More control examples will be included in another paper [10]. In the rf feedback, a fraction of the rf gap voltage is subtracted from the driving signal at an appropriate point in the amplifier chain. When using this kind of feedback with an open loop gain of H, the effective cavity impedance will be reduced by a factor $(1+H)$. For a single-harmonic system, if the rf feedback is the only control used, the threshold current in Eq. (8) can be raised by a same factor. For a double-harmonic system equipped with separate rf feedbacks for each harmonic, the linear stability conditions derived in the last section are modified by the substitution of $\mathcal{R}_k \rightarrow \mathcal{R}_k^* = \mathcal{R}_k/(1+H_k)$ for $k=1$ and 2, where H_k is the open loop gains of the rf feedbacks. Analytical relations between the stability limits and H_k are difficult to obtain in this case and a numerical evaluation is necessary.

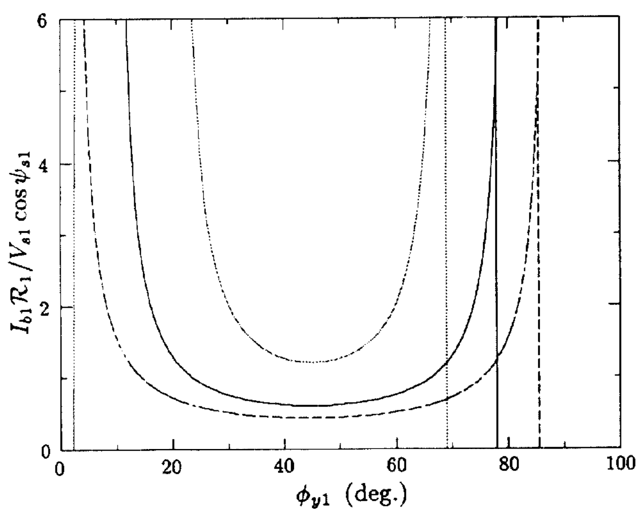

Figure 2. Plot of the threshold beam current versus ϕ_{y1} for $\mathcal{R}_2^*/\mathcal{R}_1^* = 0.8$ (dotted curves and lines), 0.4 (solid), 0.1 (dashed), and the system parameter values given in the text. The curves correspond to the solutions of $F_1 = 0$. The almost vertical lines on both sides of the curves are the solutions of $F_4 = 0$ (the LHS and the RHS solutions). For $\mathcal{R}_2^*/\mathcal{R}_1^* = 0.1$ and 0.4, the LHS solutions coincide with the line $\phi_{y1} = 0$. The stable zones are these regions below the curves and between the LHS and the RHS solutions. The thresholds derived from $F_2 > 0$ and $F_3 > 0$ are higher than 100.

As an example, consider an rf system operated at both the fundamental and the second harmonics. We assume that, in the absence of feedback, the system is characterized by $\xi = 0.8$, $Q_1 = Q_2$, $\phi_{y2} = 70°$, $\vartheta = 0.65$, $(\omega_s/\alpha_1)^2 = 0.1$, and $\mathcal{R}_2/\mathcal{R}_1 = 0.4$. With the feedback on, the threshold beam currents normalized by $(V_{s1}/\mathcal{R}_1)\cos\psi_{s1}$, are shown in Figure 2 as functions of ϕ_{y1} for the cases of $\mathcal{R}_2^*/\mathcal{R}_1^* = 0.8$, 0.4, and 0.1.

As shown in Figure 2, the stability limit given by the vertical line on the right hand side of the figure moves towards a higher detuning angle when the ratio $\mathcal{R}_2^*/\mathcal{R}_1^*$ decreases. In the medium and low ϕ_{y1} regions, the stability limit given by the curve increases as the ratio $\mathcal{R}_2^*/\mathcal{R}_1^*$ increases. Thus, for systems operated at high ϕ_{y1}, H_2 needs to be higher than H_1 in order to increase the system stability. For the systems operated at medium and low ϕ_{y1}, it may be more desirable to have higher H_1 for higher stability.

V. CONCLUSIONS

Using an equivalent circuit model and linearized circuit equations, we derived the stability conditions for the beam-loading in synchrotrons or storage rings with a higher rf harmonic. We found that, when compared with the beam-loading stability limit of a single-frequency system, the addition of higher-harmonic rf without any external control may decrease the stability threshold. Numerical examples of the stability limits were given and compared with the analytical results. The agreements between the analytical and the numerical solutions in describing the local stability are very good. Finally, we gave an example of the use of the "rf feedback" control was discussed by using an example.

VI. REFERENCES

[1] K. W. Robinson, Report No. CEA-11, Cambridge Electron Accelerator, Cambridge, Mass. (1956).

[2] H. Frichholtz et al., CERN Internal Report CERN-ISR-RF-TH/DL/77-41 (1977).

[3] Y. Miyahara et al., *Nucl. Instrum. and Methods*, **A260**, 518 (1987).

[4] See the references in: T. F. Wang, *Particle Accelerators*, **34**, 105 (1990).

[5] A. Hofmann and S. Myers, *Proc. of the XIth Intl. Conf. on High Energy Accelerators*, 610 (1980).

[6] F. Pedersen, *IEEE Trans. Nucl. Sci.*, Vol. NS-32, No. 5, 2138 (1985).

[7] T. F. Wang, *Proc. of the XVth Intl. Conf. on High Energy Accelerators*, 1097 (1992).

[8] T. F. Wang, Los Alamos National Laboratory Accelerator Theory Note AT-7:ATN-92-11 (1992).

[9] E. J. Routh, *A Treatise on the Dynamics of a System of Rigid Bodies* (Macmillan, 1877).

[10] T. F. Wang, Los Alamos National Laboratory Accelerator Theory Note. In preparation.